International Journal of World Economic Research
ISSN: 3080-9886 (Print), ISSN: 3080-9894 (Online) | Vol. 1, No. 1, 2026

Gas desorption mechanism of difficult to drain coal: experimental study based on pore-particle size coupling effect

Yuanyuan Liu [1, 2, *]

[1] Institute of Resources & Environment, Henan Polytechnic University, Jiaozuo 454000, China
[2] Henan International Joint Laboratory for Unconventional Energy Geology and Development, Henan Polytechnic University, Jiaozuo 454000, China

[*] **Corresponding author Email:** 1392606454@qq.com

Abstract: In this paper, the control mechanism of pore structure and particle size distribution on gas desorption behavior is revealed through pore fracture structure characterization, isothermal pressure desorption test and field gas extractable quantity investigation. (1) When the gas pressure is lower than 0.3 MPa, the particle size of the coal sample and the gas desorption show an abnormal relationship. Although the desorption rate of the small particle size coal sample is fast and the desorption amount is large, the residual gas content is higher, and the residual amount is reversed at the 0.3 MPa pressure point. When the pressure drops below 0.2 MPa, the non-extractable amount of coal samples with two particle sizes exceeds 3 m3/t.(2) The difference in gas adsorption and desorption characteristics of coal samples with different particle sizes is due to pore structure : specific surface area dominates adsorption capacity (5 mm particle size coal sample has stronger adsorption capacity), while pore distribution regulates desorption efficiency-macropores promote initial desorption rate (20 mm particle size coal sample has slow initial desorption rate), micropore volume determines residual gas content under relatively low pressure conditions (5 mm particle size coal sample has high residual gas content), and mesopores affect desorption continuity through equilibrium diffusion resistance.

Keywords: High metamorphic coal; Gas desorption; Pore structure; Particle size effect; Gas drainage.

1. Introduction

Gas resources are abundant in the world and are clean energy. Its development and utilization are of great significance to alleviate energy shortage and optimize energy structure[1, 2]. In the process of coal mining, gas accumulation is the main cause of major safety accidents such as gas explosion and coal and gas outburst, which seriously threatens the safety of miners and mine production efficiency [3, 4]. Therefore, gas extraction is a key means to realize gas resource utilization and reduce greenhouse gas emissions, and is also an important measure to ensure safe production of coal mines[5-7] . Through efficient gas extraction technology, gas can be converted into clean energy, providing important support for global energy transformation and sustainable development[8].

Due to tight texture, high-metamorphic coal seams usually show low permeability, gas drainage is difficult and inefficient[9, 10] . At present, the research on high-metamorphic hard-to-drain coal seams mainly focuses on how to improve coal seam permeability [11]. Common methods include hydraulic fracturing[12-14] , CO2 fracturing[15, 16] , acid fracturing[17, 18] , liquid nitrogen freeze-thaw[19, 20] and other technologies. However, for low permeability and strong adsorption coal bodies, as long as the permeability of coal seam is increased and the desorption process of gas is ignored, it is difficult to realize efficient gas extraction[21-23] .

The desorption process of gas in coal directly affects the diffusion and seepage of gas [24] , which is closely related to the strong adsorption, complex pore structure and particle size of coal[25]. The metamorphic degree affects the pore fracture structure of coal and directly affects the adsorption and desorption performance of gas [26-30]. The proportion of micropores in high-metamorphic coal is very large, and it is in closed or semi-closed state, which affects the connectivity between pores. This pore system is conducive to gas adsorption and accumulation, but not conducive to gas desorption and diffusion, increasing the risk of gas disaster formation [31-33]. Meanwhile, fine particles are easy to form during coal mining and crushing, and the unevenness of particle size effect will lead to difficult gas desorption process and reduce overall desorption efficiency[34]. At present, the mechanism of pore structure and particle size affecting gas desorption behavior is not clear, which becomes a key scientific problem restricting the production efficiency of high metamorphic coal seam.

Through literature review and field collection, about 400 groups of coal seam gas content test data were obtained from low metamorphic lignite to high metamorphic anthracite, and 314 groups of anthracite data collected were sorted out to analyze gas extractable content (Qextractable) and gas non-extractable content (Qnon-extractable), and establish correlation model in combination with vitrinite reflectance (R0), as shown in Figures 1 and 2. Figure 1 shows significant positive correlation between gas non-extractable amount and coal rank evolution. The higher the coal rank, the higher the residual gas content in coal seam; especially in the high-metamorphic coal interval (Ro,max>2.0), the pore structure in coal is complex, the non-extractable gas content is the highest, and the data correlation is strong. This also directly determines the difficult desorption characteristics of high metamorphic coal gas. Figure 2 shows that high metamorphic coal (Ro,max>2.0) non-extractable gas accounts for 52-68%, which directly determines the difficult extraction characteristics of high metamorphic coal gas, indicating that

high metamorphic coal is difficult to absorb and extract.

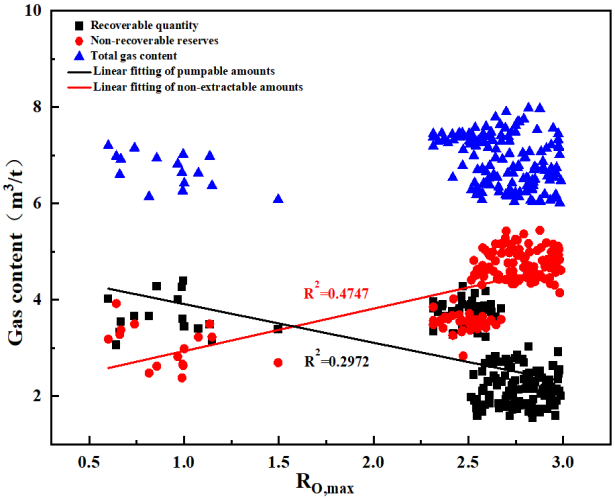

Figure 1. Relationship between vitrinite reflectance Ro and gas content

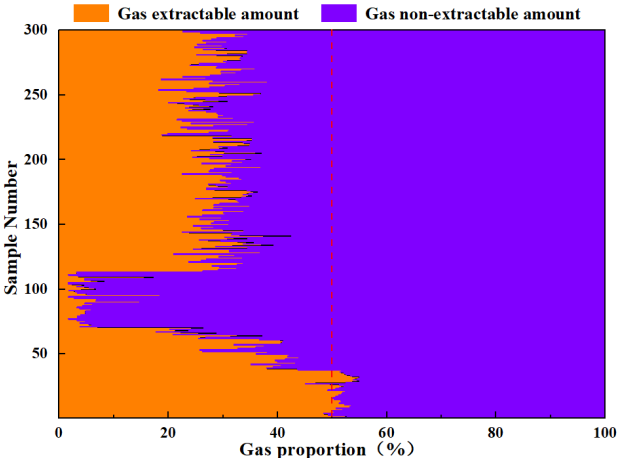

Figure 2. Distribution of extractable and non-extractable gas content in anthracite coal

In view of this, this paper takes the high metamorphic anthracite of Chensilou Coal Mine in Yongxia Kuangqu as the research object, through experiment and theoretical analysis, systematically studies the influence of pore characteristics and particle size distribution on gas desorption, reveals the gas desorption law of high metamorphic coal seam difficult to be drained, deeply studies the control mechanism of low permeability and strong adsorption of coal body on gas migration, and provides new control countermeasures for optimizing gas drainage technology. It has important theoretical and practical significance to realize mine safety production and improve energy utilization efficiency.

2. Experimental

2.1. Sample

This sample is taken from Coal Seam 22 of Chensilou Coal Mine in Yongxia Kuangqu, Carboniferous Permian Coal Field, North China (Fig.3). Fresh block samples are collected from underground coal mine, sealed and transported to laboratory. Basic parameters of coal sample are measured. Moisture, ash, volatile matter and fixed carbon content of coal sample are 1.80%, 13.48%, 10.99% and 73.73% respectively. The contents of kaolinite, quartz, anhydrite and calcite are 91.43%, 3.19%, 3.17% and 1.12% respectively, and the maximum vitrinite reflectance is 3.12%. The volatile matter, fixed carbon content and maximum vitrinite reflectance show that the coal is anthracite. In order to reduce the experimental error, the coal samples are mainly bright coal.

The raw coal samples were prepared into 60-80 mesh, 5 mm and 20 mm grain size coal samples for pore fracture structure measurement and isothermal depressurization desorption experiment, 5 mm and 20 mm lump coal samples for high pressure mercury injection experiment, 60-80 mesh coal samples for low temperature liquid nitrogen experiment, and 5 mm and 20 mm grain size coal samples for isothermal depressurization desorption experiment.

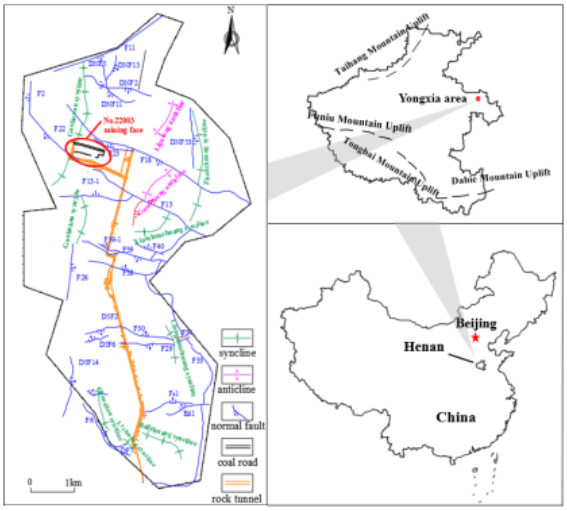

Figure 3. Geological overview map of sample collection

2.2. Pore structure measurement

Based on the prepared coal samples, the key parameters of pore structure of coal samples were obtained by high pressure mercury intrusion. Micromeritics AutoPore IV 9505 mercury intrusion instrument was used for high pressure mercury intrusion experiment. As shown in Figure 4, the relationship between pressure and pore diameter was obtained from Washburn equation.

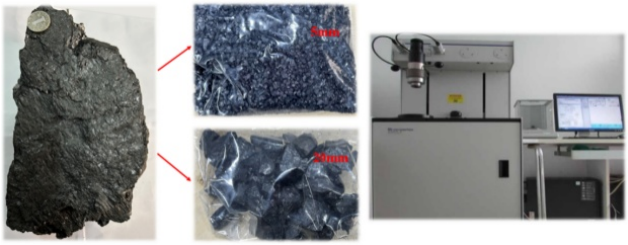

Figure 4. Micromeritics AutoPore IV 9505 mercury porosimeter was used in the experiment

2.3. Gas desorption experiment

The isothermal desorption experiment was carried out by IS-100 isothermal adsorption instrument produced by TerraTek Company of America. The experimental system mainly consists of four parts: aeration device, temperature control system, isothermal adsorption system and data acquisition and processing system, as shown in Figure 5. The specific test steps are as follows: (1) Set the temperature control system to the formation temperature of 29℃.(2) Put the coal samples with 5 mm and 20 mm particle sizes into the sample tank respectively, and fill methane after vacuumizing to make the coal samples fully adsorbed and equilibrated under the condition of 1.5 MPa.(3) The equilibrium pressure was decreased gradually (interval 0.1~0.2 MPa, interval 8 h)

until it was reduced to atmospheric pressure.(4) The system pressure and gas desorption amount were collected by computer in real time. After the experiment, the data were processed. According to Langmuir monolayer molecular adsorption model, the isothermal pressure reduction desorption curve was obtained, and the characteristics of the curve were further analyzed.[35].

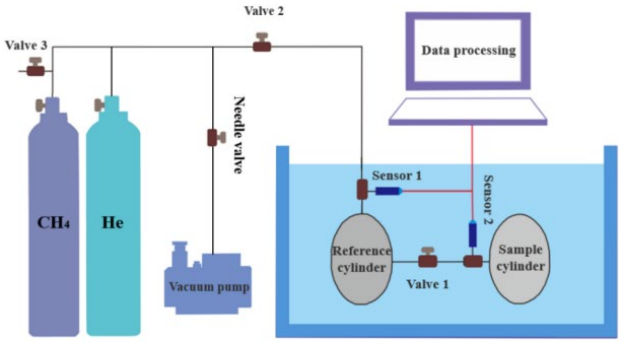

Figure 5. Methane adsorption / desorption experimental system[36]

3. Results and discussion

3.1. Mercury intrusion test results analysis

Figure 6(a) and (b) show that mercury injection curves of coal samples with particle size of 20 mm begin to coincide when pore diameter is less than 100 nm, cumulative pore volume rises rapidly and steadily, and then hysteresis loop disappears, indicating that transition pores and micropores of coal samples are mostly semi-open pores with poor pore connectivity; pore volume accumulation is significant when pore diameter is greater than 100 nm, mercury injection curves begin to appear wider hysteresis loop, indicating that medium pores and large pores of coal samples are mostly open pores with good pore connectivity; Figure 6(c) and (d) show that mercury injection curve and mercury regression curve of coal sample with grain size of 5 mm almost coincide, and hysteresis loop is small, reflecting poor pore connectivity and complex pore structure.

Figure 7(a) shows that the pore volume distribution of coal sample with particle size of 20 mm presents the characteristics of "single peak and multiple peaks" at each stage: the main peak is located in the macropore interval (> 1000nm), indicating that the macropore connectivity is high, and there are multiple gentle sub-peaks in the pore diameter range of 100-1000nm, reflecting the regulation of capillary action by transitional pores; the pore volume decreases sharply in the area with pore diameter <100 nm, indicating that the pore contribution is low and the adsorption pores are few at this stage. Figure 7(b) shows coal sample with grain size of 5mm, and pore volume distribution at different stages presents "single peak" characteristics: main peak concentrates in macropore interval (>1000 nm), indicating high macropore connectivity; pore diameter has no obvious secondary peak in the range of 100-1000 nm, reflecting limited development of transitional pores; pore volume in the area with pore diameter <100 nm has almost no contribution, indicating less adsorption pores.

Figure 8(a) shows that when the pore diameter of 20 mm coal sample is less than 10 nm, the curve rises sharply, indicating that the adsorption sites on the microporous surface are dense; when the pore diameter is more than 10 nm, the curve decreases slowly and tends to be flat, and the specific surface area contribution is low. Figure (b) shows that the coal sample with 5 mm particle diameter shows the same trend as the coal sample with 20 mm particle diameter.

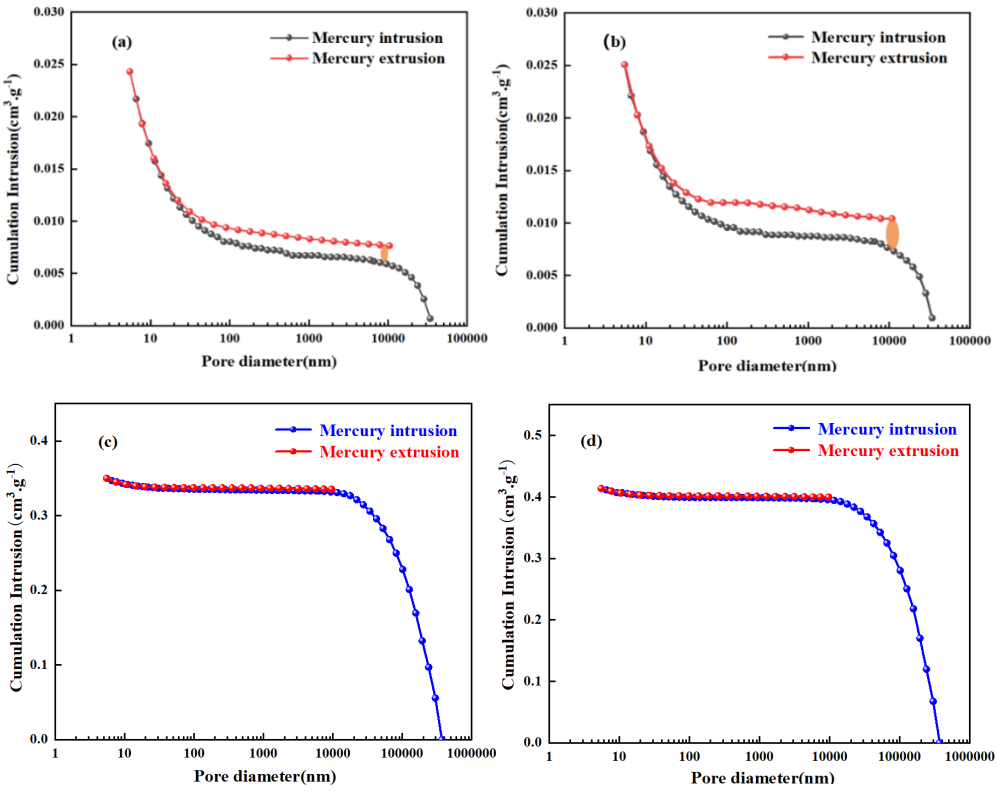

Figure 6. Curves of injection and withdrawal mercury

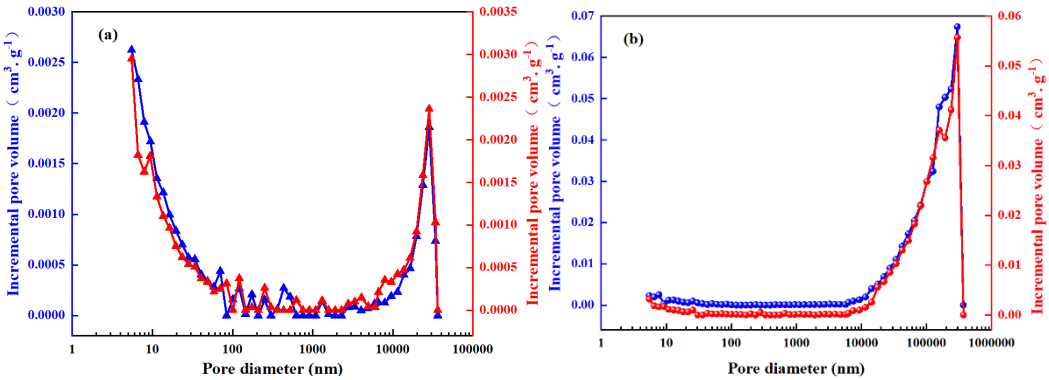

Figure 7. Distribution of pore volume with high pressure mercury injection

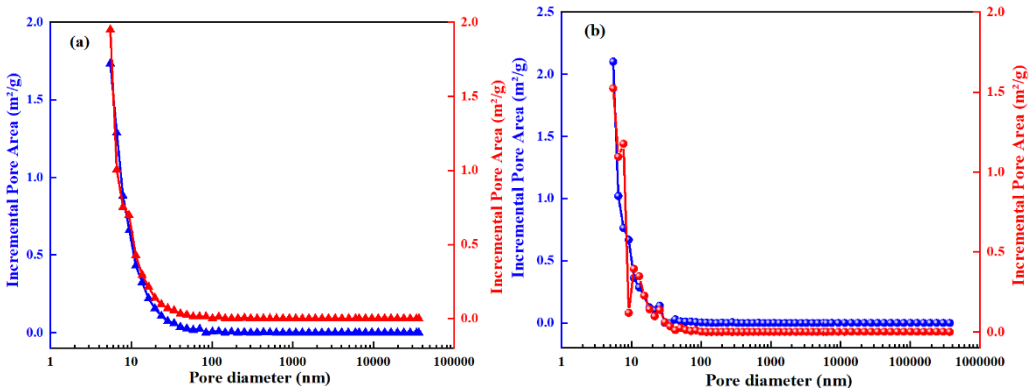

Figure 8. Distribution of surface area with high pressure mercury injection

3.2. Pore proportion analysis

In order to better characterize the pore characteristics of coal samples, the pore size range measured by high pressure mercury intrusion method is divided into four types according to the Hodot classification method, namely, macropores (> 1000 nm) and mesopores(100-1000 nm), mesopores (10-100 nm) and micropores (<10 nm)[37], respectively plot the proportion of pore volume and specific surface area of different pores of 5 mm and 20 mm grain size coal samples, red represents 20 mm grain size coal sample, blue represents 5 mm grain size coal sample.

Tables 1 and 2 show that the total pore volume and total pore surface area of coal sample with 20 mm particle size are 0.0255 cm3/g and 6.836 m2/g respectively; the average pore diameter is 14.90 nm; the proportion of micropores, transition pores, mesopores and macropores in pore volume is about 35%,30%, 3% and 30% respectively; the proportion of micropores, transition pores, mesopores and macropores in specific surface area is 25%, 24%, 0.3% and 0.03% respectively. The total pore volume and total pore surface area of 5 mm coal sample are 0.3500 cm3/g and 5.902 m2/g respectively; the average pore diameter is 237.21 nm; the proportion of micropores, transitional pores, mesopores and macropores in pore volume is about 2%, 2%, 0.2% and 95% respectively; the proportion of micropores, transitional pores, mesopores and macropores in pore specific surface area is 73%, 25%, 0.1% and 0.3% respectively.

Table 1. Mercury intrusion porosimetry parameters of coal sampl

particle size of coal sample (mm)	Total pore volume (cm3·g−1)	Total pore surface area (m2·g−1)	Average pore diameter (nm)
5	0.3500	5.902	237.21
20	0.0255	6.836	14.90

Table 2. The proportion of pores in coal samples

	Particle size of coal sample (mm)	Pore Diameter (nm)			
		micropores	mesoporous	mesoporous	macropores
Proportion of pore volume (%)	5	2	2	0.2	95
	20	35	30	3	30
Specific surface area ratio (%)	5	73	25	0.1	0.3
	20	25	24	0.3	0.03

Figure 9 (a)(b) shows that the pore volume of coal sample with 20 mm grain size is mainly microporous (<10 nm), accounting for 32%, and the proportion of macropores (>1000 nm) is moderate, accounting for about 30%; Figure 9 (c)(d) shows that the pore volume of coal sample with 5 mm grain size is mainly macroporous (>1000 nm), accounting for 95%, and the pore volume of microporous (<10 nm) is relatively low, accounting for 2%.

Figure 10 (a)(b) shows that the specific surface area of coal sample with 20 mm particle size is dominated by micropores, accounting for 75%, and transition pores account for 25%. Figure 9 (c)(d) shows that the specific surface area of coal

sample with 5 mm particle size is dominated by micropores, accounting for 75%, and transition pores account for 25%. Both cases are the same, and adsorption pores account for about 90%.

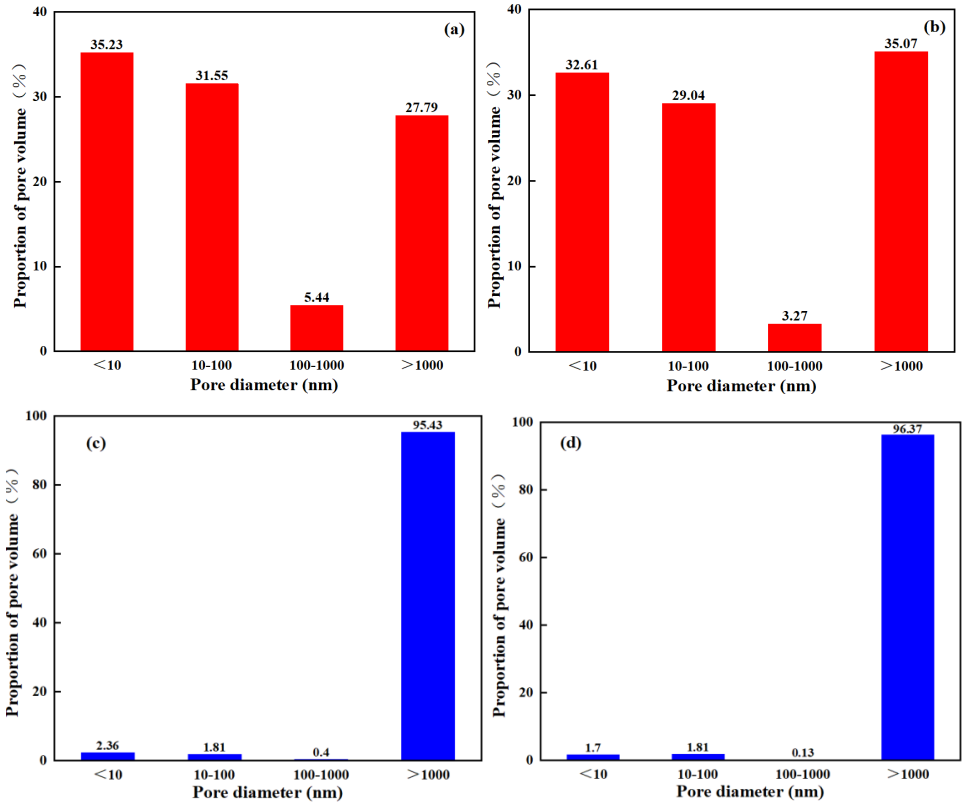

Figure 9. The distribution of pore size and stage pore volume of two kinds of coal samples under high pressure mercury injection

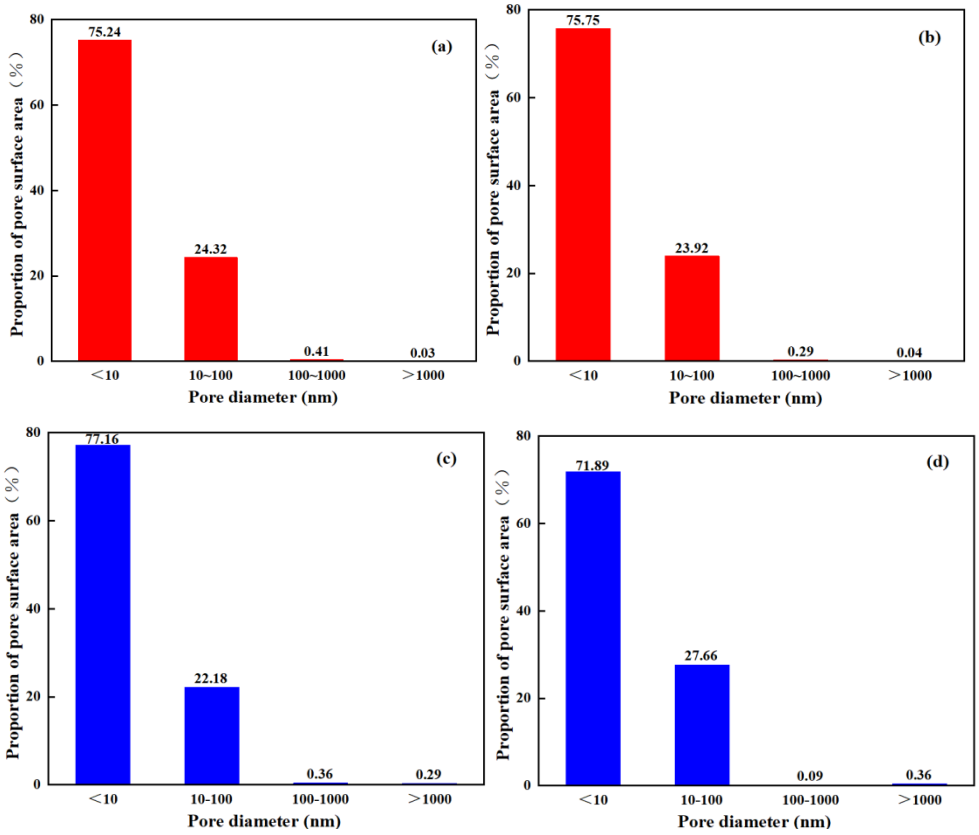

Figure 10. The distribution of pore size and stage surface area of two kinds of coal samples under high pressure mercury injection

3.3. Effect of particle size on gas desorption law of coal

Two isothermal pressure reduction desorption parallel tests are conducted on the test coal samples, as shown in Figure 11(a) and (b).(1) When the gas pressure is reduced to less than 0.2 MPa, the maximum non-extractable amount in 5 mm and 20 mm coal particles is greater than 3m3/t, corresponding to actual production, even if the coal seam gas pressure is reduced to less than 0.2 MPa, there is still 3 m3/t gas that

cannot be desorbed;(2) The desorption rate of small particle size coal samples is always greater than that of large particle size coal samples;(3) Figure (a) and (b) shows that the gas residual amount reversal phenomenon occurs at the gas pressure of 0.3 MPa in both experiments. When the pressure is lower than 0.3 MPa, the smaller the particle size, the larger the gas desorption amount and the more the residual gas content.

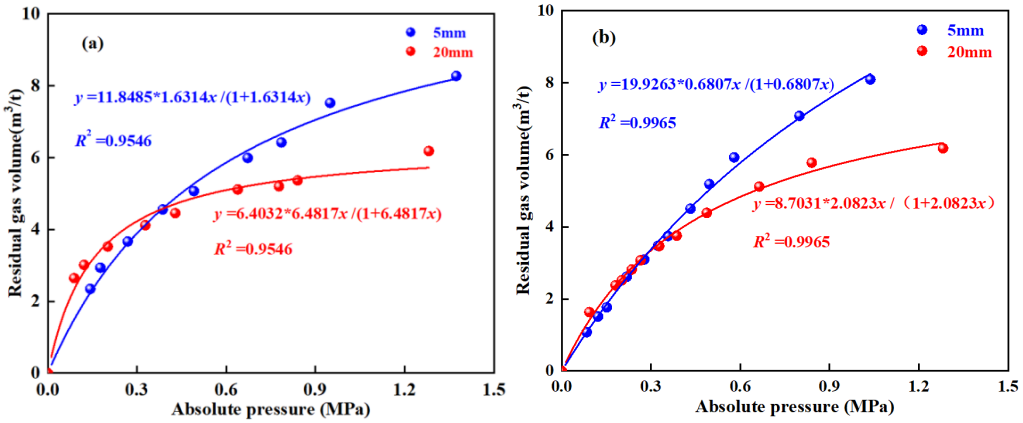

Figure 11. Desorption curve of coal sample

3.4. Effect mechanism of pore-particle size coupling on gas desorption

The pore structure and particle size distribution of high-metamorphic and difficult-to-drain coal seam can analyze the gas desorption control mechanism from both microscopic and macroscopic scales. The adsorption-desorption equilibrium dominated by micropores is restricted by surface roughness and diffusion path; particle size differentiation is the main reason for inconsistent desorption dynamics and poor overall drainage efficiency. The "pore-particle size coupling control model" is shown in Figure 12.

The pore volume of 5mm coal sample is mainly macropores (>1000 nm), accounting for 95%, and the proportion of micropores (<10 nm) is very low, about 2%, but its specific surface area is micropores and micropores, that is, adsorption pores account for 90%, indicating that coal sample adsorption points are more.(>0.3 MPa), the high connectivity of large pores significantly reduces the gas desorption resistance and promotes the rapid gas desorption rate; the low pore volume leads to less gas adsorption content and relatively low pressure stage (<0.3 MPa), narrow pore of coal sample hinders gas diffusion, resulting in difficult gas absorption and significant increase of residual gas content.

The pore volume of 20mm coal sample is mainly micropores (<10 nm), accounting for 32%, the proportion of macropores (>1000 nm) is moderate, accounting for about 30%, and the specific surface area is medium micropores and micropores, i.e. adsorption pores account for 90%, indicating that there are many adsorption points in coal sample, which enhances the actual adsorption capacity of gas. The connectivity of large pores results in slower initial desorption rate, but transition pores (10-100 nm) as a transition channel to ease the diffusion resistance, so that in the relatively low pressure stage (<0.3 MPa), the gas can be gradually released. Finally, the gas adsorbed on the inner surface of the microporous gradually desorbs through the coordination of the mesopores when the pressure drops, resulting in a lower residual amount. Through the pore structure of "microporous adsorption-mesopore transition-moderate macropores", the adsorption amount of the coal sample with 20 mm particle size is relatively low at the initial stage, and the desorption efficiency is slow.

The distribution of specific surface area of two coal samples is similar, but the difference of pore volume determines different gas desorption.(>0.3 MPa), although the pore volume is small, its high specific surface area makes gas adsorbed on the surface. Under the condition of relatively low pressure, the desorption process may be hindered due to the narrow pore size and the enhancement of surface adsorption potential, resulting in the increase of gas residual amount. However, the pore volume advantage of 20 mm coal sample combined with the transition structure of mesopore promotes the continuous desorption of coal sample from relatively high pressure stage to low pressure stage. This indicates that: The adsorption capacity may be determined by specific surface area, but the desorption efficiency is controlled by pore volume distribution and connectivity. The large pore dominates the initial desorption rate, the pore volume determines the residual gas content at low pressure, and the medium pore affects the continuity of desorption process through equilibrium diffusion resistance.

"Optimization of pore connectivity" and "regulation of particle size distribution" are the main means to solve the difficult extraction problem of high-metamorphic coal seam. For the difficult extraction problem of high-metamorphic coal seam, it is found in the previous research that the permeability of coal seam can be improved by enhancing pore connectivity, for example, gas-water composite fracturing technology[38] , CO2 phase transformation fracturing[39, 40], plasma pulse dynamic load fracturing[41] ,and other technologies can be adopted; High-pressure water jet crushing[42], classification screening and backfilling[43], nano-particle surface coating[44] and other technologies can be used to accelerate desorption rate by adjusting the particle size of coal samples. The study further proves that pore structure characterization and particle size distribution have certain influence on gas desorption law of high-metamorphic and difficult-to-extract coal seam, so it provides a new theoretical basis for improving the optimization of gas extraction technology in difficult-to-extract coal seam. Compared with previous studies, this study avoids the simplification of research through the influence mechanism of pore-particle size coupling on gas desorption, and has important practical significance for improving the drainage efficiency of high-metamorphic hard-to-drain coal seam by improving pore connectivity and particle size distribution.

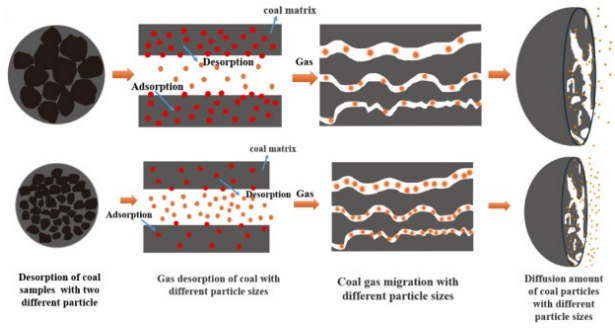

Figure 12. Mechanism diagram of pore structure and particle size on coal desorption

4. Conclusions

Gas desorption law of high metamorphic and difficult drainage coal seam is studied by pore structure characterization and particle size distribution experiment, and the influence mechanism of pore-particle size coupling on gas desorption is revealed, which provides a new theoretical basis for improving gas drainage technology optimization of difficult drainage coal seam.

(1) When the gas pressure is lower than 0.2 MPa, the maximum non-extractable amount in 5 mm and 20 mm coal particles is greater than 3 m3/t; the desorption rate of small particle size coal samples is always greater than that of large particle size coal samples; the phenomenon of gas residual amount reversal occurs at the gas pressure of 0.3 MPa in both experiments; when the gas pressure is lower than 0.3 MPa, the smaller the particle size, the larger the gas desorption amount and the more the residual gas content.

(2) The pore structure of 20 mm coal sample through "microporous adsorption-medium pore transition-moderate macropore" makes the adsorption capacity of 20 mm coal sample relatively low in the initial stage and the desorption efficiency slow; the pore structure of 5 mm coal sample "high specific surface area-low microporous volume" makes the adsorption capacity of 5 mm coal sample relatively high in the initial stage and the desorption rate fast, but the desorption efficiency is limited in the later stage, resulting in high residual gas content. The adsorption capacity is determined by specific surface area, but the desorption efficiency is controlled by pore volume distribution and connectivity. Large pores dominate the initial desorption rate, pore volume determines the residual gas content at low pressure, and medium pores affect the continuity of desorption process through equilibrium diffusion resistance.

(3) The desorption ability of high metamorphic coal seam may be affected by many factors because of its complicated geological conditions. The laboratory desorption experiment does not completely simulate the complicated underground conditions, which may underestimate the hysteresis of actual gas desorption in coal seam.

Acknowledgments

This research was supported by the National Natural Science Foundation of China (No. 42230814 and No. 42372204), the Henan Province International Science and Technology Cooperation Project (No. 242102520034), the Henan Province Science and Technology Research Project (No. 242102320365), and the Key Research Projects of Higher Education Institutions in Henan Province (No. 24B170005).

Declarations

Conflict of Interest: The authors have no competing interests to declare that are relevant to the content of this article.

References

[1] LENG K, GUAN B, LIU W, et al. Research progress of coalbed methane extraction[J]. Energy Reports, 2024,12: 5728-5746.

[2] LI S, QIN Y, TANG D, et al. A comprehensive review of deep coalbed methane and recent developments in China[J]. International Journal of Coal Geology, 2023,279: 104369.

[3] NI L, YUAN A, HU Z. Pressure–Relief Gas Cooperative Drainage Technology in a Short-Distance Coal Seam Group[J]. Applied Sciences, 2023,13(9).

[4] WARD S G. Safety in Mines Research[J]. Nature, 1958,181(4610): 676-677.

[5] CHANGBAO J, YANG Y, WENHUI W, et al. A new stress-damage-flow coupling model and the damage characterization of raw coal under loading and unloading conditions[J]. International Journal of Rock Mechanics and Mining Sciences, 2021,138.

[6] ZHOU A, HU J, WANG K. Carbon emission assessment and control measures for coal mining in China[J]. Environmental Earth Sciences, 2020,79(19): 47-56.

[7] WANG Y, LIU B, XUE S, et al. Insight into influence of degradation metabolism of Firmicutes on the microstructure of anthracite coal[J]. Energy Exploration & Exploitation, 2025,43(1): 205-225.

[8] KARACAN C Ö, RUIZ F A, COTÈ M, et al. Coal mine methane: A review of capture and utilization practices with benefits to mining safety and to greenhouse gas reduction[J]. International Journal of Coal Geology, 2011,86(2): 121-156.

[9] DU Y, SANG S, PAN Z, et al. Experimental study of supercritical CO2 -H2O-coal interactions and the effect on coal permeability[J]. Fuel, 2019,253: 369-382.

[10] JOSHI D, PRAJAPATI P, SHARMA P, et al. Past, present and future of Coal Bed Methane (CBM): a review with special focus on the Indian scenario[J]. International Journal of Coal Preparation and Utilization, 2023,43(2): 377-402.

[11] LI H, LAU H C, HUANG S. China's coalbed methane development: A review of the challenges and opportunities in subsurface and surface engineering[J]. Journal of Petroleum Science and Engineering, 2018,166: 621-635.

[12] PAN J, MOU P, JU Y, et al. Micro-nano-scale pore stimulation of coalbed methane reservoirs caused by hydraulic fracturing experiments[J]. Journal of Petroleum Science and Engineering, 2022,214: 110512.

[13] JIENAN P, PENGWEI M, YIWEN J, et al. Micro-nano-scale pore stimulation of coalbed methane reservoirs caused by hydraulic fracturing experiments[J]. Journal of Petroleum Science and Engineering, 2022,214.

[14] GUO F, LV R, SONG D, et al. Coalbed Methane Enhancement in Low-Permeability Reservoirs by Hydraulic Fracturing with Coated Ceramsite[J]. Energy & Fuels, 2023,37(13): 9023-9031.

[15] LIU G, LI B, ZHANG Z, et al. Effects of Liquid CO2 Phase Transition Fracturing on Methane Adsorption of Coal[J]. Energy & Fuels, 2023,37(3): 1949-1961.

[16] ZHANG Z, LIU G, LIN J, et al. Fractal Evolution Characteristics on the Three-Dimensional Fractures in Coal Induced by CO2 Phase Transition Fracturing[J]. Fractal and Fractional, 2024,8(5): 273.

[17] ZHOU D, LV Z, CAO Y, et al. Fractal Evolution Characteristics of Pore Structure in Coal-Acidified Stimulation[J]. Fractal and Fractional, 2025,9(2): 62.

[18] GUANHUA N, HONGCHAO X, SHANG L, et al. The effect of anionic surfactant (SDS) on pore-fracture evolution of acidified coal and its significance for coalbed methane extraction[J]. Advanced Powder Technology, 2019,30(5): 940-951.

[19] QIN L, ZHAI C, LIU S, et al. Changes in the petrophysical properties of coal subjected to liquid nitrogen freeze-thaw – A nuclear magnetic resonance investigation[J]. Fuel, 2017,194: 102-114.

[20] HAMED A, ALIREZA K, FAISAL U R A, et al. Coal cleat network evolution through liquid nitrogen freeze-thaw cycling[J]. Fuel, 2022,314.

[21] GAOFENG L, HUAN L, BAOAN X, et al. Fuzzy pattern recognition model of geological sweetspot for coalbed methane development[J]. Petroleum Exploration and Development, 2023,50(4): 924-933.

[22] LI Z, LIU D, WANG Y, et al. Evaluation of multistage characteristics for coalbed methane desorption-diffusion and their geological controls: A case study of the northern Gujiao Block of Qinshui Basin, China[J]. Journal of Petroleum Science and Engineering, 2021,204: 108704.

[23] ZHENGDONG L, XIAOSONG L, ZHENYANG W, et al. Modeling and experimental study on methane diffusivity in coal mass under in-situ high stress conditions: A better understanding of gas extraction[J]. Fuel, 2022,321.

[24] XIANGLIANG Z, SHEN J, BAIQUAN L, et al. Study on the influence of different-voltage plasma breakdowns on functional group structures in coal[J]. Energy, 2023,284.

[25] QING H, CUNBAO D, ZHIXIN J, et al. Molecular Simulation of the Adsorption Characteristics of Methane in Pores of Coal with Different Metamorphic Degrees[J]. Molecules, 2021, 26(23): 7217.

[26] GAO J, LI Z, TAO X, et al. A comprehensive study of multiscale pore structural characteristics in deep-buried coals of different ranks. [J]. Scientific reports, 2025,15(1): 8299.

[27] XIANGCHUN L, ZHONGBEI L, FAN Z, et al. Nanopore Structure of Different Rank Coals and Its Quantitative Characterization.[J]. Journal of nanoscience and nanotechnology, 2021,21(1): 22-42.

[28] REN J, SONG Z, LI B, et al. Structure feature and evolution mechanism of pores in different metamorphism and deformation coals[J]. Fuel, 2021,283.

[29] YANG Z, LI Y, XUE W, et al. Small molecules from multistep extraction of coal and their effects on coal adsorption of CH 4[J]. Catalysis Today, 2020,374(prepublish): 192-199.

[30] WANG C, FAN R, ZHANG S, et al. Pore structure modification and characterization of carbon adsorbent prepared by high-sulfur anthracite blending coal[J]. International Journal of Coal Preparation and Utilization, 2023,43(10): 1740-1758.

[31] ZHANG X, DU Z, LI P. Physical characteristics of high-rank coal reservoirs in different coal-body structures and the mechanism of coalbed methane production[J]. Science China Earth Sciences, 2016,60(2): 246-255.

[32] LU F, LIU C, ZHANG X, et al. Study on full-scale pores characterization and heterogeneity of coal based on low-temperature nitrogen adsorption and low-field nuclear magnetic resonance experiments[J]. Scientific Reports, 2024,14(1): 16910.

[33] HAO X, YUEPING Q, DAOYONG Y, et al. Experimental investigation of gas diffusion kinetics and pore-structure characteristics during coalbed methane desorption within a coal seam[J]. Gas Science and Engineering, 2024,121: 205173.

[34] ZHENYANG W, YUANPING C, LIANG W, et al. Analysis of pulverized tectonic coal gas expansion energy in underground mines and its influence on the environment.[J]. Environmental science and pollution research international, 2020,27(2): 1508-1520.

[35] ZHU W L B J. Impact of tectonic deformation on coal methane adsorption capacity[J]. Adsorption Science & Technology, 2019,37(9-10): 698-708.

[36] ZHAI Y, LI Y, SONG D, et al. Gas Diffusion Characteristics and Size Effect in Coal Particles with Different Degrees of Metamorphism[J]. Energy & Fuels, 2023,37(3): 2030-2039.

[37] DIFEI Z, YINGHAI G, GEOFF W, et al. Fractal Analysis and Classification of Pore Structures of High-Rank Coal in Qinshui Basin, China[J]. Energies, 2022,15(18): 6766.

[38] SHI B, CAO Y, LI Z, et al. Experimental Study on Permeability Enhancement of Anthracite by High Pressure Nitrogen Injection and Soaking[J]. Energy & Fuels, 2024,38(9): 7850-7861.

[39] LIU H, LIU G, ZHANG Z, et al. Effects of Liquid CO2 Phase Transition Fracturing on Mesopores and Micropores in Coal[J]. Energy & Fuels, 2022,36(17): 10016-10025.

[40] CAO Y, ZHANG J, ZHAI H, et al. CO2 gas fracturing: A novel reservoir stimulation technology in low permeability gassy coal seams[J]. Fuel, 2017,203: 197-207.

[41] AGARWAL M, KUDAPA V K. Plasma based fracking in unconventional shale – A review[J]. Materials Today: Proceedings, 2023,72: 2791-2795.

[42] WANG L, LI J, XU F, et al. Research on the high-pressure water jet impacting on the different solids based on improved SPH method[J]. Archive of applied mechanics (1991), 2024,94(2): 333-346.

[43] LI X, CHOI M, KIM K, et al. Effects of pulverized coal particle size on flame structure in a methane-assisted swirl burner[J]. Fuel, 2019,242: 68-76.

[44] M J L, LU G, WYATT S I C, et al. Elastomeric microparticles for acoustic mediated bioseparations.[J]. Journal of nanobiotechnology, 2013,11(1): 22.